J. Anat. (1994) 185, pp. 503–509, with 3 figures Printed in Great Britain

Spermatogenesis and ultrastructure of a peculiar acrosomal formation in the musk shrew, *Suncus murinus*

M. KUROHMARU[1], H. KOBAYASHI[1], S. HATTORI[2], T. NISHIDA[3] AND Y. HAYASHI[1]

[1] *Department of Veterinary Anatomy, Faculty of Agriculture, University of Tokyo,* [2] *Institute of Medical Science, University of Tokyo, and* [3] *Laboratory of Anatomy and Physiology, Department of Animal Husbandry, College of Agriculture and Veterinary Medicine, Nihon University, Fujisawa, Japan*

(*Accepted 5 May 1994*)

ABSTRACT

Spermatogenesis and acrosomal formation in the musk shrew, *Suncus murinus*, were studied by light and transmission electron microscopy. The cycle of the seminiferous epithelium was divided into 13 stages based on the characteristics of acrosomal change and nuclear shape, appearance of meiotic figures, location of spermatids, and period of spermiation. The relative frequencies of stages 1 to 13 were 5.1, 5.9, 10.1, 8.8, 12.5, 11.5, 10.6, 7.9, 6.0, 4.8, 8.9, 3.1 and 4.8, respectively. Additionally, spermatid development was subdivided into 13 steps. Acrosomal formation during spermiogenesis in the musk shrew was quite characteristic. However, in contrast to other mammalian species, the nucleus remained in the middle region of the seminiferous epithelium, and only the acrosome extended towards the basement membrane, beginning at step 7. The extension of the acrosome was conspicuous and reached maximum at step 9. At that time, the tip of the acrosome extended nearly to the basement membrane. The acrosome of maturing spermatids was about 3-fold longer than that of spermatozoa. Thereafter, the acrosome gradually shortened and became flat. The enormous fan-shaped acrosome was completely formed at step 13. The prominent extension and subsequent shortening and flattening of the acrosome in the musk shrew appears to be a unique process to form the enormous fan-shaped acrosome.

Key words: Spermatozoa; seminiferous epithelium; spermatids.

INTRODUCTION

Several investigations describe spermatogenesis in various mammalian species (Monesi, 1962; Swierstra & Foote, 1963; Clermont & Harvey, 1965; Swierstra, 1968; Tiba et al. 1968; Foote et al. 1972; Kennelly, 1972; Clermont & Antar, 1973; Swierstra et al. 1974; Grocock & Clarke, 1975; Schuler & Gier, 1976; Oud & De Rooij, 1977; Ekstedt et al. 1986; Osman & Plöen, 1986; Kurohmaru et al. 1988). Although it is accepted that spermatozoa in some insectivores possess a peculiar fan-shaped acrosome (Cooper & Bedford, 1976; Green & Dryden, 1976; Koehler, 1977; Mori & Uchida, 1985), little information is available on spermatogenesis in insectivores. In a previous study (Adachi et al. 1992), we tried to clarify spermatogenesis in Watase's shrew, *Crocidura watasei*, a small insectivore on the Nansei islands in Japan, using light and transmission electron microscopy. We found that acrosomal formation in Watase's shrew was quite characteristic. However, during spermiogenesis, the acrosome extended prominently towards the basement membrane of the seminiferous epithelium. It then gradually shortened and became flat. This extreme change in shape has not so far been found in other mammalian species. Future investigations of other shrew species are required to analyse development of this peculiar acrosomal shape. The musk shrew, an Insectivore, is easily obtained for research in Japan as it was developed more than 10 years ago as an experimental animal. The present study examined musk shrew testes by light and transmission electron microscopy to classify the stages of the seminiferous epithelium, to clarify the ultrastructure of acrosomal

Correspondence to Dr M. Kurohmaru, Department of Veterinary Anatomy, Faculty of Agriculture, The University of Tokyo, Bunkyo-ku, Tokyo 113, Japan.

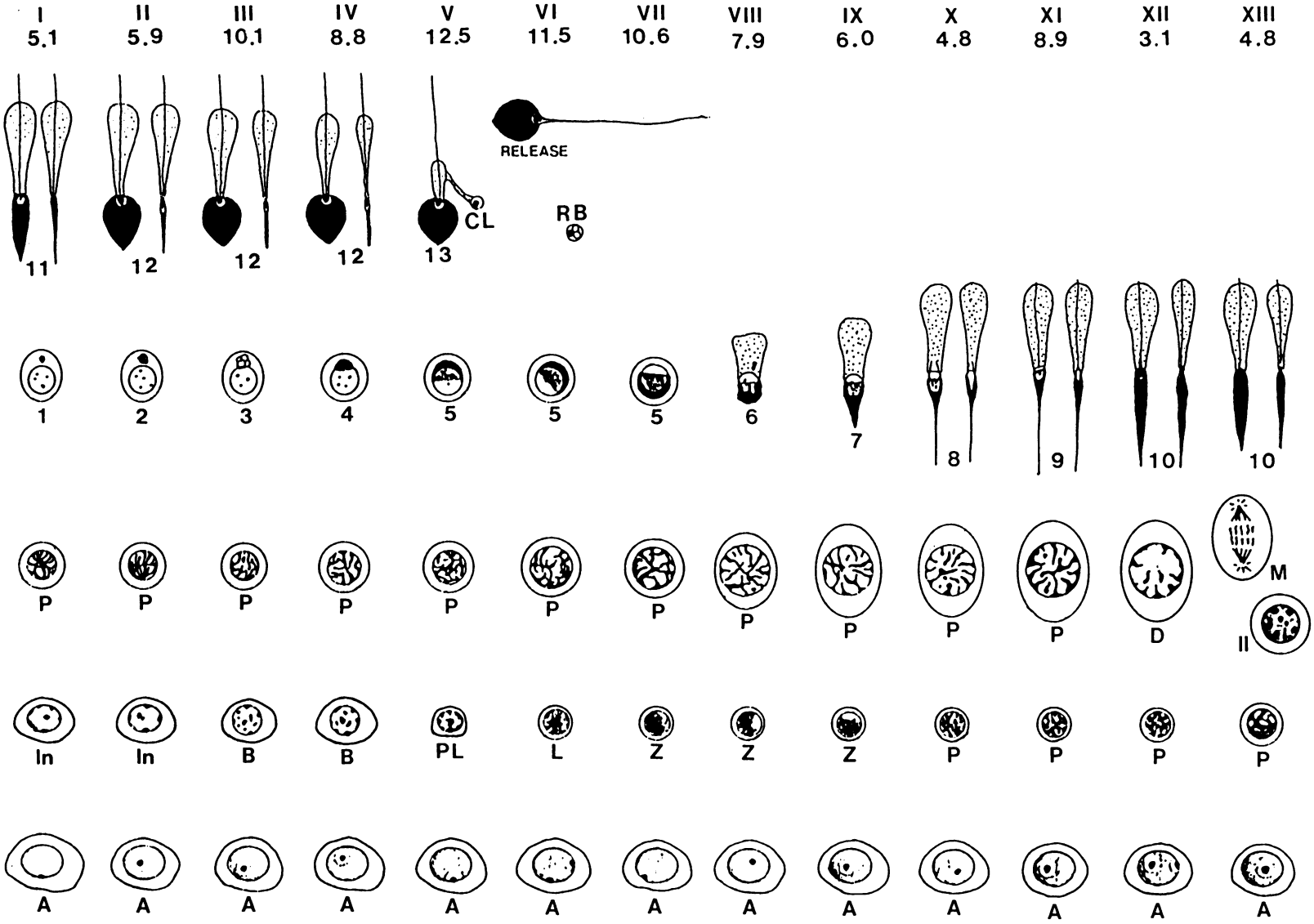

Fig. 1. Schematic drawing of the cycle of the seminiferous epithelium in the musk shrew. A, In, B, differentiated spermatogonia; PL, L, Z, P, D, primary spermatocytes; PL, preleptotene phase; L, leptotene phase; Z, zygotene phase; P, pachytene phase; D, diplotene phase; II, secondary spermatocyte; M, meiotic figure. Roman numerals represent each stage. Arabic numerals beneath the Roman numerals show the relative frequency of each stage as a percentage. Arabic numerals beneath each spermatid show each step. CL, cytoplasmic lobe; RB, residual body.

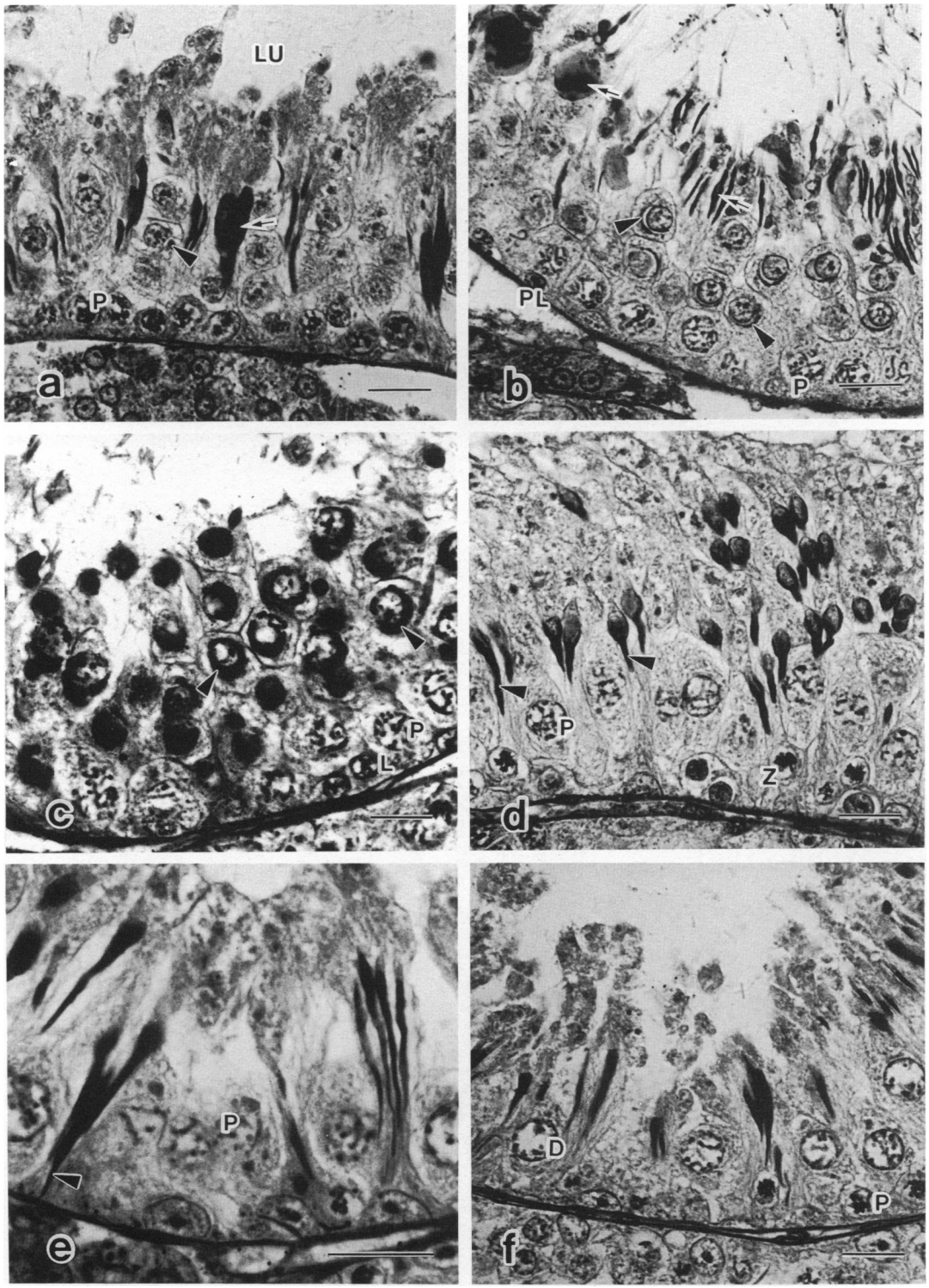

Fig. 2. Light micrographs of seminiferous tubules at each stage. (*a*) Stage I. Two generations of spermatids are present in the seminiferous epithelium. The tip of maturing spermatids with a flat acrosome (arrow) is located in the middle region of the epithelium. An idiosome (arrowhead) is observed in the vicinity of the nucleus of early round spermatids. LU, lumen; P, pachytene spermatocyte. (*b*) Stage V. At this stage, 2 generations of spermatids are still detected. Mature spermatids at step 13 (arrows) are arranged along the luminal surface of the epithelium. Acrosomes (arrowheads) cover half of the nuclear surface of round spermatids. P, pachytene spermatocyte; PL, preleptotene spermatocyte. (*c*) Stage VI. After mature spermatids are released into the lumen, only one generation of spermatids is present in the epithelium. The acrosome (arrowheads) surrounds more than half of the spermatid nucleus. L, leptotene spermatocyte; P, pachytene spermatocyte. (*d*) Stage IX. The acrosome (arrowheads) is extending towards the base of the epithelium. The spermatid nucleus is slightly elongated. P, pachytene spermatocyte; Z, zygotene spermatocyte. (*e*) Stage XI. Extension of the acrosome (arrowhead) reaches maximum at this stage. The tip of the acrosome approaches the basement membrane. The spermatid nucleus remains located in the middle region of the epithelium. P, pachytene spermatocyte. (*f*) Stage XII. The acrosome begins to shorten. The width of the acrosome tends to increase in accordance with its shortening. D, diplotene spermatocyte; P, pachytene spermatocyte. Bar, 20 μm.

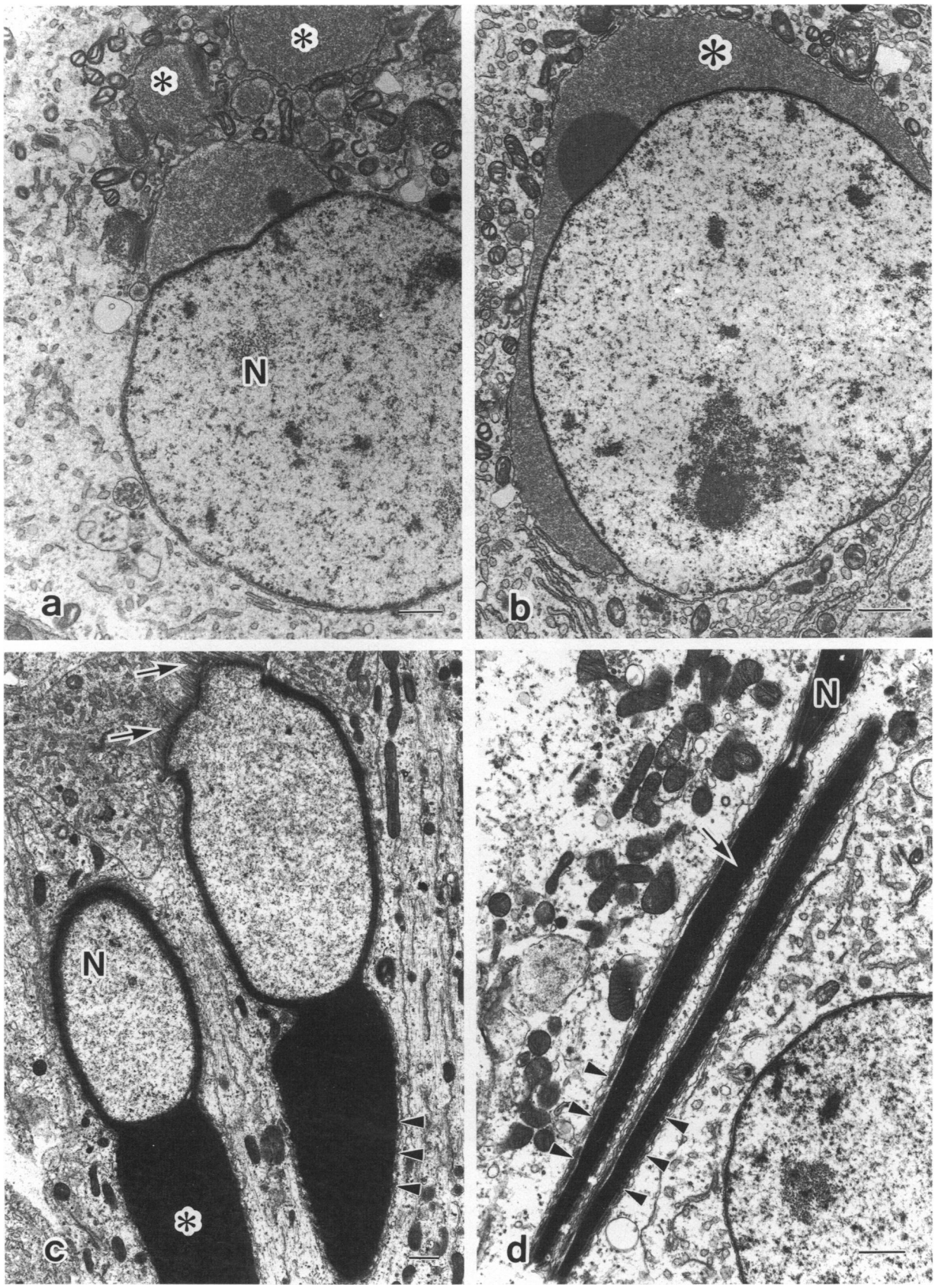

Fig. 3. Transmission electron micrographs of developing spermatid. (*a*) Spermatid at step 4. The acrosome is obvious on the nuclear surface of the round spermatid. Some acrosomal granules (asterisks) are present remote from the acrosome. A well developed Golgi complex is seen in the vicinity of the acrosomal area. N, nucleus. (*b*) Spermatid at step 5. The acrosome (asterisk) covers more than half of the nuclear surface. The Golgi complex is still recognisable near the acrosome. (*c*) Spermatid at step 7. The acrosome (asterisk) extends towards the basement membrane. Sertoli/spermatid junction (ectoplasmic specialisation, arrowheads) is detectable around the acrosome. The spermatid nucleus (N)

formation, and to compare results with those in Watase's shrew and other mammalian species previously studied.

MATERIALS AND METHODS

Fifteen adult male musk shrews, 40–74 g in weight, were used in the present study. Most of the animals were obtained from the Department of Anatomy, Nippon Medical School, the Department of Pharmacology, the University of Tokyo and Central Institute for Experimental Animals. Some were captured on Tokunoshima island. No differences in spermatogenic features were found among these animals.

Light microscopy

Under ether anaesthesia, the testes of 10 musk shrews were excised surgically and immersed in Bouin's fixative. Samples were cut into slabs, dehydrated in a graded series of ethanol, and embedded in paraffin. Sections (4–5 μm) were stained with periodic acid Schiff (PAS)-haematoxylin and observed by light microscopy. Fifty round seminiferous tubules which showed only one stage were selected from each testis. A total of 100 round seminiferous tubules (50 tubules × 20 testes) was evaluated and classified into each stage.

Whole mount samples were also prepared according to Clermont & Bustos-Obregon (1968) for discriminating type B in spermatogonia and preleptotene spermatocytes. After removing the tunica albuginea, the detached seminiferous tubules from 2 musk shrews were immersed in Bouin's fixative for 2–3 h. The tubules were placed in 3 consecutive baths containing 80% ethanol, 70% ethanol, and distilled water, respectively. They were then stained with haematoxylin, dehydrated in a graded series of ethanol, mounted on a glass, and observed by light microscopy.

Transmission electron microscopy

Under pentobarbital anaesthesia, the testes of 3 musk shrews were perfused through the thoracic aorta with Ringer's solution followed by 2.5 or 5% glutaraldehyde in 0.1 M phosphate buffer. The testes were excised surgically, cut into smaller pieces and immersed in the same fixative. After washing with phosphate buffer, they were postfixed in 1% osmium tetroxide in 0.1 M phosphate buffer, dehydrated in a graded series of ethanol and embedded in Quetol 812. Thick sections (approximately 1 μm) were stained with toluidine blue and observed by light microscopy. Thin sections were stained with uranyl acetate and lead citrate and observed with a JEM-100S or JEM-1200EX transmission electron microscope at 80 kV.

RESULTS

The cycle of the seminiferous epithelium

The cycle of the seminiferous epithelium in the musk shrew was divided into 13 stages on the basis of acrosomal changes, nuclear shape, appearance of meiotic figures, location of spermatids, and period of spermiation. The characteristic acrosomal changes of spermatids were mainly used as a criterion. The relative frequencies of stages 1 to 13 were 5.1, 5.9, 10.1, 8.8, 12.5, 11.5, 10.6, 7.9, 6.0, 4.8, 8.9, 3.1 and 4.8, respectively (Fig. 1).

Division of type B spermatogonia at stage V produced primary spermatocytes at preleptotene phase (Fig. 2*b*), and they grew into the leptotene phase at stage VI (Fig. 2*c*). Leptotene primary spermatocytes were present at only one stage and changed into zygotene spermatocytes at stage VII. Zygotene primary spermatocytes were observed from stages VII to IX (Fig. 2*d*). Pachytene primary spermatocytes developed from zygotene spermatocytes and first appeared at stage X. From stages X to XII (Fig. 2*f*), 2 kinds (early, late) of pachytene spermatocytes were detected within the seminiferous epithelium. Pachytene primary spermatocytes were recognisable throughout all stages. They gradually developed and divided into secondary spermatocytes at stage XIII. Meiotic figures were observed frequently at this stage. Secondary spermatocytes divided to produce an early round spermatid that first appeared at stage I (Fig. 2*a*). It contained a PAS-positive acrosomal vesicle within the cytoplasm. The acrosomal vesicle gradually developed and attached to the nuclear membrane at stage III. A maturing elongated spermatid was also detected at stage I (Fig. 2*a*). Two generations of spermatids, an early round spermatid and a maturing flattened spermatid, were present until stage V (Fig. 2*b*). The acrosome was apparently formed on the nuclear surface of the round spermatid

is partly elongated. The manchette (arrows) is clearly seen in the upper part of the figure. (*d*) Spermatid at step 12. The spermatid nucleus (N) is condensed. ES (arrowheads) surrounds the whole acrosomal surface. The extended acrosome is still embedded within the Sertoli cell crypt. Bars, 1 μm.

at stage IV and then expanded to cover half of the nuclear surface at stage V (Fig. 2*b*). The acrosomal tip of the round spermatid rotated to face the basement membrane of the tubule at stage VII. After stage VIII, the elongation of the round spermatid nucleus progressed to some extent. During this process, flattening of the spermatid nucleus was more conspicuous than elongation. The nucleus began to condense after stage X. The acrosome extended towards the basement membrane after stage IX (Fig. 2*d*), whereas the spermatid nucleus remained situated in the middle region of the epithelium. The acrosome reached maximum extension at stage XI (Fig. 2*e*). At that time, the acrosome of maturing spermatids was about 3-fold longer than that of spermatozoa. The apical tip of the acrosome was located close to the basement membrane at this stage. Thereafter, the acrosome gradually shortened and became flat. At stages II–V, the acrosome revealed a fan-like shape. At stage VI (Fig. 2*c*), the matured spermatid with a fan-shaped acrosome was released from the epithelium (spermiation).

Ultrastructure of acrosomal formation during spermiogenesis

Spermatid development was subdivided into 13 steps by light microscopic observation (Fig. 1). Steps 1–3, 4–5, 6–11 and 12–13 of the spermatid corresponded to the Golgi, cap, acrosome and maturation phases, respectively.

At step 1, a few acrosomal vesicles were present in the vicinity of the spermatid nucleus. Thereafter, the vesicles fused with each other to increase in diameter. Although one large vesicle attached to the nuclear membrane at step 3, some vesicles were still present away from the nucleus. During the Golgi phase (steps 1–3), a well developed Golgi complex was located close to the vesicles. During steps 4 (Fig. 3*a*) and 5 (Fig. 3*b*), the acrosome that was formed at step 3 spread over the nuclear surface to cover half of the nucleus. At step 6 when the spermatid rotated and its anterior pole faced the base, the outer membrane of the acrosome converged upon the plasma membrane of the spermatid. At step 7 (Fig. 3*c*), the acrosome began to extend towards the basement membrane. The manchette, consisting of bundles of microtubules, was clearly seen at this step. The microfilament bundles also were obviously detected at ectoplasmic specialisation (ES; Russell, 1977) sites between the Sertoli cell and spermatid. Thereafter, the acrosome with ES gradually extended towards the base and reached maximum length at step 9. Even at this step, the surface of the extended acrosome was completely surrounded by ES. After step 10, the acrosome showed a tendency to shorten. Accompanying the progress of shortening, the acrosome gradually became flattened from steps 11–12 (Fig. 3*d*). The shortening and flattening of the acrosome were completed at step 13. Mature spermatids (step 13) with an enormous fan-shaped acrosome were arranged along the apical surface of the epithelium.

DISCUSSION

Spermatogenesis in the musk shrew is fundamentally similar to that in the Watase's shrew and other mammalian species, with some exceptions. The cycle of the seminiferous epithelium in the Watase's shrew is divided into 12 stages, while the cycle in the musk shrew is composed of 13 stages. The extension of the acrosome towards the basement membrane (stages VIII–XI) takes a longer period in the musk shrew than in Watase's shrew. From the beginning of acrosome extension to the maximum, it takes 3 steps in the musk shrew, but only 2 in Watase's shrew. In fact, the extension of the acrosome is more remarkable in the musk shrew. This finding may explain the difference in the number of stages between the 2 species. During the Golgi phase (steps 1–3), the Golgi complex is well developed within the spermatid cytoplasm of the musk shrew. The conspicuously developed Golgi complex must contribute to the early formation of the large acrosome.

The process of acrosomal formation during spermiogenesis in the musk shrew is quite characteristic. In other mammalian species examined to date (Foote et al. 1972; Kennelly, 1972; Grocock & Clarke, 1975; Kurohmaru et al. 1988), both the acrosome and the elongating nucleus of the spermatid gradually move to the basal region of the seminiferous tubule and subsequently migrate in the opposite direction towards the lumen prior to spermiation. In contrast, during the same process the spermatid nucleus of the musk shrew remains located in the middle region of the seminiferous epithelium, and only the acrosome extends towards the basement membrane. Although a similar process is observed in Watase's shrew (Adachi et al. 1992), the extension of the acrosome is more conspicuous in the musk shrew. When the acrosome shortens it does not seem to change in quantity: the width increases to correspond with the decrease in length. The prominent extension and subsequent shortening and flattening of the acrosome in the musk and Watase's shrews appear to be required to form the enormous fan-shaped acrosome. This peculiar

acrosomal formation was not observed in the European common shrew, *Sorex araneus*, which possesses a relatively smaller acrosome (Plöen et al. 1979) compared with that of the musk shrew. The findings suggest that this unique process of acrosomal formation may be common only in shrews with an enlarged fan-shaped acrosome.

The significance and mechanism of the movement of elongating spermatids between the luminal side and the basal region still remain unresolved. More detailed investigations of the peculiar acrosomal formation in the musk shrew may provide new insight into this phenomenon. Furthermore, corresponding to acrosome extension, ES also extends towards the basement membrane to a considerable degree. The musk shrew may be a useful model to clarify the function and structure of ES.

ACKNOWLEDGEMENTS

We wish to thank the Department of Anatomy, Nippon Medical School and the Department of Pharmacology, University of Tokyo, for provision of the animals. This work was supported in part by a Grant-in-Aid for Scientific Research Fund from the Ministry of Education, Science and Culture, Japan.

REFERENCES

ADACHI Y, KUROHMARU M, HATTORI S, HAYASHI Y (1992) Spermatogenesis in the Watase's shrew, *Crocidura watasei*. A light and electron microscopic study. *Experimental Animal* **41**, 295–303.

CLERMONT Y, HARVEY S (1965) Duration of the cycle of the seminiferous epithelium of normal, hypophysectomized and hypophysectomized-hormone treated albino rats. *Endocrinology* **76**, 80–89.

CLERMONT Y, BUSTOS-OBREGON E (1968) Re-examination of spermatogonial renewal in the rat by means of seminiferous tubules mounted 'in toto'. *American Journal of Anatomy* **122**, 237–248.

CLERMONT Y, ANTAR M (1973) Duration of the cycle of the seminiferous epithelium and the spermatogonial renewal in the monkey. *Macaca arctoides*. *American Journal of Anatomy* **136**, 153–166.

COOPER GW, BEDFORD JM (1976) Asymmetry of spermiation and sperm surface charge patterns over the giant acrosome in the musk shrew *Suncus murinus*. *Journal of Cell Biology* **69**, 415–428.

EKSTEDT E, SÖDERQUIST L, PLÖEN L (1986) Fine structure of spermatogenesis and Sertoli cell (*Epithellocytus sustentans*) in the bull. *Anatomia Histologia Embryologia* **15**, 23–48.

FOOTE RH, SWIERSTRA EE, HUNT WL (1972) Spermatogenesis in the dog. *Anatomical Record* **173**, 341–352.

GREEN JA, DRYDEN GL (1976) Ultrastructure of epididymal spermatozoa of the Asiatic musk shrew, *Suncus murinus*. *Biology of Reproduction* **14**, 327–331.

GROCOCK CA, CLARKE JR (1975) Spermatogenesis in mature and regressed testes of the vole (*Microtus agrestis*). *Journal of Reproduction and Fertility* **43**, 461–470.

KENNELLY JJ (1972) Coyote reproduction: I. The duration of the spermatogenic cycle and epididymal sperm transport. *Journal of Reproduction and Fertility* **31**, 163–170.

KOEHLER JK (1977) Fine structure of spermatozoa of the Asiatic musk shrew, *Suncus murinus*. *American Journal of Anatomy* **149**, 135–152.

KUROHMARU M, TIBA T, NISHIDA T, HAYASHI Y (1988) Spermatogenesis and ultrastructural changes of spermatids during spermiogenesis in the cotton rat, *Sigmodon hispidus*. *Okajimas Folia Anatomica Japonica* **65**, 203–220.

MONESI V (1962) Autoradiographic study of DNA synthesis and the cell cycle in spermatogonia and spermatocytes of mouse testis using tritiated thymidine. *Journal of Cell Biology* **14**, 1–18.

MORI, T, UCHIDA T (1985) Fine structure of the spermatozoa of the house musk shrew, *Suncus murinus*. In *Suncus murinus, Biology of the Laboratory Shrew* (ed. K. Kondo), pp. 335–351. Tokyo: Japan Scientific Societies Press (in Japanese).

OSMAN DI, PLÖEN L (1986) Spermatogenesis in the camel (*Camelus dromedarius*). *Animal Reproduction Science* **10**, 23–26.

OUD JL, DE ROOIJ DG (1977) Spermatogenesis in the Chinese hamster. *Anatomical Record* **187**, 113–124.

PLÖEN L, EKWALL H, AFZELIUS BA (1979) Spermiogenesis and the spermatozoa of the European common shrew (*Sorex araneus* L). *Journal of Ultrastructural Research* **68**, 149–159.

RUSSELL LD (1977) Observations on rat Sertoli ectoplasmic ('junctional') specializations in their association with germ cells of the rat testis. *Tissue & Cell* **9**, 475–498.

SCHULER HM, GIER HT (1976) Duration of the cycle of the seminiferous epithelium in the prairie vole (*Microtus ochrogaster ochrogaster*). *Journal of Experimental Zoology* **197**, 1–12.

SWIERSTRA EE (1968) Cytology and duration of the cycle of the seminiferous epithelium of the boar; duration of spermatozoan transit through the epididymis. *Anatomical Record* **161**, 171–186.

SWIERSTRA EE, FOOTE RH (1963) Cytology and kinetics of spermatogenesis in the rabbit. *Journal of Reproduction and Fertility* **5**, 309–322.

SWIERSTRA EE, GEBAUER MR, PICKETT BW (1974) Reproductive physiology of the stallion. I. Spermatogenesis and testis composition. *Journal of Reproduction and Fertility* **40**, 113–123.

TIBA T, ISHIKAWA T, MURAKAMI A (1968) Histologische Unterschung der Kinetik der Spermatogenese beim Mink (*Mustela vison*). I. Samenepithelzyklus in der Paarungszeit. *Japanese Journal of Veterinary Research* **16**, 73–87.